AGU PUBLICATIONS

Geophysical Research Letters

RESEARCH LETTER
10.1002/2016GL068432

Key Points:
- We use observed ozone-temperature relationships and extreme value theory to predict future ozone
- An unexpected 20% of U.S. sites show ozone suppression at extremely high temperatures
- Results from CMIP5 imply increases in U.S. ozone episodes by as much as 3–9 days by the 2050s

Supporting Information:
- Supporting Information S1

Correspondence to:
L. Shen,
lshen@fas.harvard.edu

Citation:
Shen, L., L. J. Mickley, and E. Gilleland (2016), Impact of increasing heat waves on U.S. ozone episodes in the 2050s: Results from a multimodel analysis using extreme value theory, *Geophys. Res. Lett.*, *43*, doi:10.1002/2016GL068432.

Received 29 FEB 2016
Accepted 9 MAR 2016
Accepted article online 15 MAR 2016

Impact of increasing heat waves on U.S. ozone episodes in the 2050s: Results from a multimodel analysis using extreme value theory

L. Shen[1], L. J. Mickley[1], and E. Gilleland[2]

[1]School of Engineering and Applied Sciences, Harvard University, Cambridge, Massachusetts, USA, [2]Research Applications Laboratory, National Center for Atmospheric Research, Boulder, Colorado, USA

Abstract We develop a statistical model using extreme value theory to estimate the 2000–2050 changes in ozone episodes across the United States. We model the relationships between daily maximum temperature (T_{max}) and maximum daily 8 h average (MDA8) ozone in May–September over 2003–2012 using a Point Process (PP) model. At ~20% of the sites, a marked decrease in the ozone-temperature slope occurs at high temperatures, defined as ozone suppression. The PP model sometimes fails to capture ozone-T_{max} relationships, so we refit the ozone-T_{max} slope using logistic regression and a generalized Pareto distribution model. We then apply the resulting hybrid-extreme value theory model to projections of T_{max} from an ensemble of downscaled climate models. Assuming constant anthropogenic emissions at the present level, we find an average increase of 2.3 d a^{-1} in ozone episodes (>75 ppbv) across the United States by the 2050s, with a change of +3–9 d a^{-1} at many sites.

1. Introduction

Temperature is the most important meteorological factor in driving ozone episodes in polluted regions [e.g., *Camalier et al.*, 2007; *Jacob and Winner*, 2009, and references therein; *Porter et al.*, 2015]. *Lin et al.* [2001] found that the probability of ozone exceeding a threshold increases with temperature; for example, during 1980–1998, the probability of daily maximum 8 h average (MDA8) ozone exceeding 85 ppbv was 20% at 303 K and 49% at 310 K in New England. More recently, high summer temperatures in the central United States in 2012 led to values of the annual fourth MDA8 ozone of 78.0 ppbv, more than 8 ppb higher than the 2008–2014 average of 69.8 ppbv (http://www3.epa.gov/airtrends/ozone.html). The 2012 enhancement occurred even though emissions of ozone precursors have declined dramatically in recent years [*Kim et al.*, 2006; *Bloomer et al.*, 2009]. In the coming decades, global climate change will likely cause more frequent and/or persistent heat waves in the United States [*Meehl and Tebaldi*, 2004; *Steiner et al.*, 2010; *Gao et al.*, 2013; *Wu et al.*, 2014], and a key question is whether such trends will increase the frequency or severity of ozone episodes. In this study we develop a statistical model based on extreme value theory (EVT) to calculate the 2000–2050 changes in temperature-driven ozone episodes at sites across the United States.

Surface ozone is produced via oxidation of volatile organic compounds and CO in the presence of nitrogen oxides (NO_x), and the relationship of ozone with temperature arises from a set of complex chemical and biophysical mechanisms. In the eastern United States, surface ozone typically shows a linear relationship with surface temperature with slopes ranging from 2 to 6 ppbv/°C in the Northeast and Midwest, depending on emissions and meteorological regime [*Camalier et al.*, 2007; *Bloomer et al.*, 2009; *Rasmussen et al.*, 2012; *Sillman and Samson*, 1995]. At extreme temperatures, however, the linear relationship between temperature and ozone can change. For example, *Steiner et al.* [2010] diagnosed suppression of ozone formation at high temperatures at sites in California. These authors hypothesized that suppression arises from (1) reduced isoprene emission due to biophysical constraints at high temperatures and (2) saturation of ozone formation from the decomposition of peroxyacetyl nitrate (PAN), a reservoir of NO_x. To date, the phenomenon of ozone suppression has not been reported elsewhere in the United States. In this study, we look for evidence of ozone suppression at high temperatures outside of California.

Most previous efforts examining the climate penalty on future ozone episodes have relied on chemical transport models or chemistry climate models (CCMs) [e.g., *Wu et al.*, 2008; *Gao et al.*, 2013; *Rieder et al.*, 2015], but such models have difficulty in capturing present-day ozone variability [e.g., *Fiore et al.*, 2009; *Doherty et al.*, 2013; *Parrish et al.*, 2014]. An alternative method is to use a statistical approach. Most previous statistical approaches for calculating surface ozone assumed linear relationships between ozone and the driving

meteorological variables [e.g., *Schlink et al*., 2003; *Holloway et al*., 2008; *Chang et al*., 2014]. *Rieder et al*. [2013], however, pointed out that the extreme tails of surface ozone data are typically non-Gaussian, so linear regression likely underpredicts the present-day number of exceedances. An alternative representation of extreme ozone events takes advantage of extreme value theory (EVT). Instead of fitting the entire data set, EVT focuses on accurate simulation of extreme ozone tails. For example, *Rieder et al*. [2013] used EVT by applying a stationary generalized Pareto distribution (GPD) model to MDA8 ozone levels at sites across the United States. That study found that 1 year ozone return levels dropped by over 8 ppbv from 1988–1998 time period to 1999–2009 in the eastern United States. Applying GPD to the future ozone simulated by a CCM, *Rieder et al*. [2015] found that climate change could increase the 1 year return level of MDA8 ozone in the east by ~1 ppbv by the 2100 s. The GPD model is appropriate in modeling the ozone distribution over a high threshold but cannot provide information on exceedance rates.

In contrast, the point process (PP) model, another approach, can simulate both the distribution above a specified threshold and the rate of exceeding this threshold. Here we apply PP to model the observed relationships between surface temperature and MDA8 ozone in May–September over 2003–2012. A novel feature of our approach is that it takes into account the possible suppression of ozone concentrations at extreme temperatures. The resulting hybrid-EVT model incorporates the nonstationarity of the ozone-temperature relationship. To calculate ozone exceedances in the 2050s, we apply our model to projections from an ensemble of climate models. Use of the ensemble increases confidence in our results.

2. Data

We obtain the 2003–2012 hourly ozone from the EPA Air Quality System (EPA-AQS, http://www.epa.gov/ttn/airs/airsaqs/) and convert it to daily maximum 8 h average (MDA8) ozone. The ozone season is defined as the period from May to September, when ozone episodes are most frequent [*Bloomer et al*., 2009]. We also compare the results in AQS with those in the EPA Clean Air Status and Trends Network (CASTNet, http://epa.gov/castnet/). Sites missing more than 10% of the data in this time frame are discarded, resulting in 816 AQS sites and 67 CASTNet sites across the United States.

The daily maximum temperature (T_{max}) is from the North American Regional Reanalysis (NARR), with a grid resolution of 32 km × 32 km [*Mesinger et al*., 2006]. CASTNet includes site-based hourly temperatures, so we use NARR temperature data to interpret only the AQS measurements. Future projections of daily maximum temperature are from the Coupled Model Intercomparison Project Phase 5 (CMIP5), under the representative concentration pathway (RCP) 4.5 scenario [*Taylor et al*., 2012]. The original CMIP5 outputs are available only at coarse horizontal resolution (e.g., ~200 km). In order to capture the fine-scale features of atmospheric circulation, we use the Bias-Correction and Constructed Analogues (BCCA) data set, which includes meteorological variables statistically downscaled from the CMIP5 ensemble [*Maurer and Hidalgo*, 2008]. The BCCA database has a grid resolution of 1/8° × 1/8° (http://gdo-dcp.ucllnl.org/downscaled_cmip_projections/) [*Bureau of Reclamation*, 2013]. Here we use the BCCA daily maximum temperatures from an ensemble of 19 CMIP5 models for the 2000–2009 and 2050–2059 time periods (Table S1 in the supporting information).

3. Observed Ozone Suppression

In this study, we define ozone suppression as a marked decrease in the ozone-temperature slope that occurs at high temperatures. To diagnose suppression, we check the stationarity of the ozone-temperature slopes at each AQS and CASTNET site using the *Z* test, as in *Paternoster et al*. [1998]. More specifically, we test whether there is a break in the slopes, with slopes in the higher-temperature regime significantly less than the slopes in the lower temperature regime. The formula of the *Z* test is given by

$$Z = \frac{m_H - m_N}{\sqrt{\mathrm{SE}_H^2 + \mathrm{SE}_N^2}} \tag{1}$$

where the m_H and m_N are the ozone-temperature slopes at high- and normal-temperature regimes, respectively, and SE_H and SE_N are the standard errors of the slopes associated with the two regimes.

For each site, we first rank all daily T_{max} values across the 10 years. We then test a series of temperature values, in increments of 0.1 K from the 95th to 97.5th percentile range, for the cutoff temperature T_x, above which

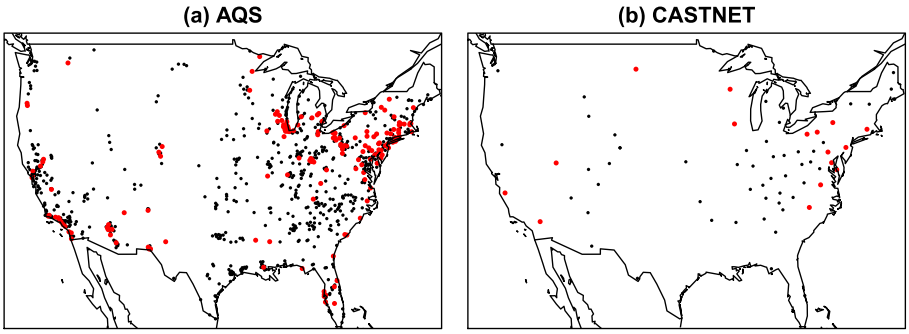

Figure 1. Distribution of EPA sites exhibiting "ozone suppression" at high temperatures in the (a) AQS and (b) CASTNET data sets during May to September for 2003–2012. Red points denote sites with significant ozone suppression at the $p < 0.05$ level, and black points are all other sites.

ozone suppression occurs. Of the candidate T_x values for each site, we choose the one that yields the minimum p value for E1. The total number of observations at each site varies from 1377 to 1530, depending on the fraction of missing data. A p value < 0.05 for E1 implies a significant reduction in slope, which we take as evidence of ozone suppression at high temperatures at that site. Figure 1 identifies those sites exhibiting ozone suppression in the AQS and CASNET networks over 2003–2012, with high similarity in the spatial distributions between these two networks. About 20% of the sites in AQS and 23% of sites in CASTNET show significant ozone suppression. Besides California, ozone suppression occurs in ~37% of sites in the Northeast, ~30% of sites in the Midwest, and a few sites in the deep South. By testing with different temperature data sets and different preprocessing methods (Text S1 and Figure S1), we confirm that the spatial distribution of ozone suppression in Figure 1 is robust.

For California, a region with relatively frequent days with T_{max} exceeding 310 K, *Steiner et al.* [2010] proposed two mechanisms to explain the observed ozone suppression. First, they posit that isoprene emissions may be reduced above 310 K due to denaturation at high temperatures of the enzymes needed for isoprene production [*Guenther et al.*, 1993]. Second, they suggest that the temperature effect on the lifetime of PAN, an important reservoir for NO_x, diminishes at very high temperatures, with ozone production leveling off.

We find that reduction in isoprene emissions at higher temperatures is unlikely to explain the observed ozone suppression in the Northeast and Midwest. In these regions, the change in slope of ozone-temperature occurs below ~305 K (Figure S2). The leaf temperatures at which the isoprene-temperature relationship flattens or reverses show large interspecies variability, but all are greater than 308 K [*Guenther et al.*, 1993; *Sharkey et al.*, 1996; *Singsaas and Sharkey*, 2000; *Rasulov et al.*, 2010]. The leaf-air temperature difference depends on many environmental variables, but at air temperatures above 306 K, the leaf temperature tends to be lower than air temperature [*Idso et al.*, 1981; *Andrews et al.*, 1992]. Taken together these observations suggest that the isoprene suppression is unlikely to occur at air temperatures of ~305 K and the cause of ozone suppression in the Northeast and Midwest must lie elsewhere.

We turn to a chemistry model GEOS-Chem to test whether the decrease in PAN lifetime in high-temperature regimes can account for ozone suppression across the United States. The details of model setup can be found in Text S2. We conduct two 9 year simulations for May–September from 2004 to 2012, a control simulation and a sensitivity simulation. In both simulations, we test for ozone suppression as described above. The control simulation (*C*) yields evidence of ozone suppression at high temperatures in grid squares across the West, Midwest, and Northeast, but not in the Southeast (Figure 2a). GEOS-Chem also diagnoses ozone suppression in the Intermountain West and northern Great Plains, where few observations exist. In the sensitivity simulation (*S*), surface air temperatures are increased everywhere by 1 K in the model. This adjustment affects only the chemistry processes and biogenic emissions but has no effect on other meteorological fields. The ozone-temperature slopes at each site in high-temperature and more normal temperature regimes can be written as

$$\begin{aligned} m_H^* &= O_{S,H} - O_{C,H} \\ m_N^* &= O_{S,N} - O_{C,N} \end{aligned} \tag{2}$$

where O represents the daily MDA8 ozone concentrations averaged over the high (H, > 95th percentile) and normal (N, 50th to 95th percentiles) temperature regimes; m_H^* and m_N^* represent the change in ozone per

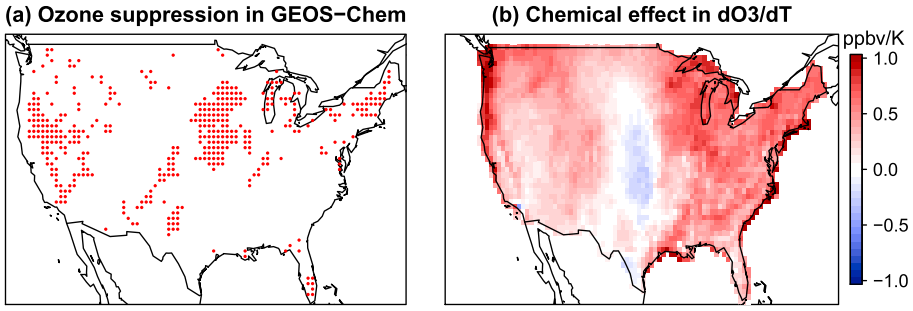

Figure 2. (a) Simulated ozone suppression in GEOS-Chem (May–September 2004–2012). Red points denote sites exhibiting significant ozone suppression at the $p < 0.05$ level. (b) Difference in the slope dO_3/dT for two temperature regimes, high (> 95th percentile) and normal (50th to 95th percentiles). The slopes are calculated by applying a uniform 1 K increase in surface temperatures in a sensitivity simulation. Positive values show where modeled dO_3/dT is greater in the high-temperature regime than in the normal regime. Negative values show the opposite and reveal where the model predicts that ozone suppression at high temperatures takes place due solely to photochemical effects.

unit temperature for these two regimes; and *C* and *S* refer to the two simulations. If ozone suppression in the model occurs due to temperature alone, m_H^* should be less than m_N^*. Figure 2b, however, reveals only weak ozone suppression at high temperatures in the southern Great Plains.

Our results suggest that ozone suppression is not caused by temperature-dependent effects in chemistry or emissions as hypothesized by *Steiner et al.* [2010] but instead arises from meteorological processes that accompany high surface temperatures. Typically, ozone is linearly correlated with temperature, which, in turn, is linearly correlated with other meteorological variables such as solar radiation, synoptic circulation, and stagnation [*Jacob and Winner*, 2009, and references therein]. At high temperatures, the linearity of these correlations among meteorological variables may begin to break down, changing the ozone-temperature slope. The breakdown in such correlations would likely not be captured in a box model such as that used in *Steiner et al.* [2010]. Although 3-D chemistry models historically have had difficulty representing observed ozone variability [e.g., *Fiore et al.*, 2009; *Pfister et al.*, 2014; *Rieder et al.*, 2015], they can better capture the full suite of meteorological effects on ozone episodes.

4. Hybrid Extreme Value Model

The extreme value model is used to study the high tail of the MDA8 ozone distribution, which has greatest relevance for ozone air quality management. We model the daily MDA8 ozone concentrations conditionally on daily maximum temperature (T_{max}), using a nonstationary PP model, which formulates the Poison process limit of extreme ozone concentrations above a threshold [*Coles*, 2001; *Rieder et al.*, 2013]. More details about this model can be found in the supporting information Text S3. We estimate the model parameters by maximizing the likelihood function *L*, which is given by

$$L(\mu_{t,T}, \sigma_T, \xi) = \exp\left\{-\frac{1}{n_a}\sum_{t=1}^{n}\left[1+\frac{\xi(u-\mu_{t,T})}{\phi_T}\right]^{-1/\xi}\right\}\prod_{t=1}^{n}\left\{\frac{1}{\phi_T}\left[1+\frac{\xi(y_t-\mu_{t,T})}{\phi_T}\right]^{-1/\xi-1}\right\}^{I[y_t>u]} \quad (3)$$

$$\mu_{t,T} = f(t,T) \quad (4)$$

$$\phi_T = \exp(g(T)) \quad (5)$$

where y_t is the daily observed MDA8 ozone from each individual AQS site, n_a is the number of observations in each year, $\mu_{t,T}$ is the location parameter conditioned on both time *t* (e.g., 2003 and 2004) and daily maximum temperature *T*, $\phi_T (> 0)$ is the scale parameter conditioned on T_{max}, ξ is the shape factor, and *f* and *g* are linear functions. The value of n_a is 153, the total number of days from 1 May to 30 September. $I[y_t > u]$ is one if the observed y_t is greater than the threshold *u* (90th percentile values of ozone in this study) and zero, otherwise. The numerical optimization is carried out using the *extRemes* package in *R* [*Gilleland and Katz*, 2011]. Application of the PP model to U.S. ozone air quality requires that we take into account trends in the emissions of ozone precursors. For example, ozone levels have declined concurrently with the ~40% reduction in power plant NO_x emission in the eastern United States beginning in 2002 [*Kim et al.*, 2006; *Bloomer*

et al., 2009]. To include this trend in the PP model, we define the location parameter μ as a function of time t (E4). The responses of the scale and shape parameters to time are relatively weak, so we define the scale parameter as a function of just T_{max} (E5) and fix the shape parameter to a constant value.

Because the single PP model is optimized by considering all available observations, it functions best when the ozone-temperature relationship shows little variability across different temperature regimes. Thus, the PP model may fail to capture ozone suppression at extremely high temperatures. Here we use the generalized Pareto distribution (GPD) model to formulate the ozone distribution at those sites where ozone suppression occurs. The GPD accounts for only the intensity of values above the high threshold (u) and not the probability of ozone exceeding this threshold [*Coles*, 2001]. In order to account for the frequency of exceedances, we use a logistic regression model, which we call the hybrid-EVT model.

As an example of this problem and our approach to solving it, Figure S4a shows the distribution of mean daily MDA8 ozone concentrations and T_{max} in May–September from 2003 to 2012 in Nanticoke, PA (76.0°W, 41.2°N). The Z test described in section 3 suggests that ozone suppression occurs at $T_{max} > 303$ K. The 90th percentile ozone at this site is 70 ppbv (threshold u), and Figure S4b shows the observed and fitted fraction of ozone above this threshold, revealing a bias in modeled T_{max} above 303 K. The bias suggests that the PP model fails to capture the ozone suppression at this site. To remedy this problem, we refit the part of data above the cutoff temperature (T_x) for ozone suppression using a logistic regression and a GPD. The GPD is defined by two parameters, the scale parameter ϕ^* and the shape parameter ξ^*, while the logistic regression is defined by two parameters denoted as θ_1 and θ_2. The probability density P of ozone is defined as

$$P(y_t|T > T_x) = \underbrace{\text{logit}(T|\theta_1, \theta_2)}_{\text{logistic regression}} \underbrace{\phi_T^{*-1}\left[1 + \frac{\xi^*(y_t - u)}{\phi^*}\right]^{-1/\xi^*-1}}_{\text{GPD}} \tag{6}$$

where T_x is the cutoff temperature for observed ozone suppression, the logit$(T|\theta_1,\theta_2)$ is the probability of ozone exceeding T_x using a logistic regression conditioned on daily maximum temperature, and ϕ^* and ξ^* are the scale and shape parameters of the GPD. The number of data points characterized by ozone suppression is relatively limited, making it challenging to use a nonstationary GPD. For simplicity, we therefore use a stationary GPD with fixed scale and shape parameter. In the resulting hybrid-EVT model, the likelihood L of an ozone exceedance over the entire data set is

$$L(\mu_{t,T}, \sigma_T, \xi, \sigma^*, \xi^*, \theta_1, \theta_2) = \begin{cases} \exp\left\{-\frac{1}{n_d}\sum_{t=1}^{n}\left[1 + \frac{\xi(u - \mu_{t,T})}{\sigma_T}\right]^{-1/\xi}\right\} \prod_{t=1}^{n}\left\{\frac{1}{\sigma_T}\left[1 + \frac{\xi(y_t - \mu_{t,T})}{\sigma_T}\right]^{-1/\xi-1}\right\}^{I[y_t>u]} & (T \le T_x) \\ \text{logit}(T|\theta_1, \theta_2)\sigma_T^{*-1}\left[1 + \frac{\xi^*(y_t - u)}{\sigma^*}\right]^{-1/\xi^*-1} & (T > T_x) \end{cases} \tag{7}$$

As seen from the equation, the likelihood consists of two parts, the PP model and logistic GPD. Because these two parts are independent of each other, the maximum likelihood estimation can be divided into two independent parts, reducing the computation complexity. We perform this calculation in extRemes [*Gilleland and Katz*, 2011]. We find that the distribution of ozone in the high tails can be adequately fitted using this hybrid-EVT model. For the model evaluation, we use a tenfold cross validation, in which we use observations in 1 year as the test data and the rest as training data. This process is repeated for every year in the time series. The coefficient of determination (R^2) between annual mean observed and simulated ozone episodes across the United States is as high as 0.98, as seen in Figure S5.

5. The 2000–2050 Trend in Ozone Episode Days in RCP4.5

Increasing greenhouse gases will lead to higher temperatures across North America, with potential implications for the frequency or duration of extreme ozone episodes. Figure S6 shows the change in the mean and 99th percentile daily T_{max} values for May–September across the United States, projected by 19 downscaled CMIP5 models from 2000–2009 to 2050–2059 for RCP4.5. Mean daily T_{max} increases by 2–2.5 K over much of the North in this time frame, including the northern Intermountain West, northern Great Plains, the Midwest, and the Northeast. In the deep South and Southwest, mean daily T_{max} increases ~1.2–1.8 K.

To estimate the frequency of future ozone episodes, we apply the hybrid-EVT model to the CMIP5 future temperature projections. First, we assume the anthropogenic emissions of ozone precursors remain at the present level (2003–2012) during the 2050–2059 time frame. Second, we apply a parametric bootstrap to the hybrid-EVT model and simulate the 2003–2012 observed ozone observations 500 times. In each bootstrap step, the fitted hybrid-EVT model calculates the ozone concentration distribution as a function of T_{max} at each site for the CMIP5 historical (2000–2009) and future scenarios (2050–2059). The ozone distributions over these time frames are calculated by averaging the ozone distribution for all days. Third, we calculate the cumulative probability of ozone episode days for 2000–2009 and 2050–2059 in each model and at each site. For all sites in the East and most sites in the West, an ozone episode day is defined as a day with MDA8 ozone greater than 75 ppbv. In California, where 53 sites experience MDA8 ozone of 75 ppb more than 20% of the time, we define an ozone episode day as the 90th percentile of 2003–2012 ozone concentrations. Fourth, we calculate the mean and standard deviation in the changes of ozone episode days across the 19 CMIP5 models at each site. These metrics can be written as

$$\overline{\Delta x} = \frac{\sum_{i=1}^{19}\sum_{j=1}^{n}\Delta x_{i,j}}{19n} \tag{8}$$

$$\sigma_{\text{total}} = \sqrt{\frac{\sum_{i=1}^{19}\sum_{j=1}^{n}\left(\Delta x_{i,j} - \overline{\Delta x}\right)^2}{19n}} \tag{9}$$

where $\Delta x_{i,j}$ is the changes in ozone episode days by 2050s in the ith ($1 \le i \le 19$) model and jth ($1 \le j \le n$) bootstrap simulations, $\overline{\Delta x}$ is the average change in ozone episode days across all models and all bootstrap simulations, and σ_{total} is the standard deviation across all models and bootstrap simulations.

Figure 3a shows the predicted changes in the number of ozone episode days in May–September from 2000–2009 to 2050–2059. We find that the number of episode days increases by an average of 2.3 days across all sites in the United States from 2000 to 2050, with many sites in the California, Northeast, and Great Lakes regions revealing increases of 3 to 9 d a^{-1}, with the relative change ranging from 40% to 100%. This spatial distribution of projected ozone exceedance days arises from two causes. First, the present-day number of ozone episodes is already large in some regions (e.g., Northeast, Midwest, and Southwest, Figure S3a), implying a greater potential for more frequent ozone episodes as temperatures rise. Second, as shown in Figure S6, the Northeast, Midwest, and southern California regions all experience more frequent extreme temperatures in the future atmosphere, driving relatively large increases in ozone episode days in these areas. Changes in ozone episode days in the Southeast, however, are generally below 1 d a^{-1} or even negative. This result is consistent with Figure S3, which shows that surface ozone in the Southeast is relatively insensitive to changes in T_{max} or even exhibits a negative response to increasing T_{max} [*Camalier et al*., 2007; *Bloomer et al*., 2009; *Wu et al*., 2008; *Porter et al*., 2015]. In addition, the projected increases in temperature in the Southeast are 1–2 K less than elsewhere in the United States (Figure S6).

Figure 3b shows the total standard deviation (σ_{total}, E9) calculated from the 19 projections in different CMIP5 models over all bootstrap simulations. The uncertainty is greatest in the Northeast and Southwest, reaching 2–5 d a^{-1}, but much less in other regions, showing a similar spatial pattern with the average changes of ozone episodes in Figure 3a. We further decompose the total standard deviation into two parts: the internal part caused by uncertainty of the parameters in the hybrid-EVT model and the external part caused by different temperature projections (Text S4). As seen from Figure S7, the external standard deviation is much greater than the internal one in the Northeast, Midwest, and California, suggesting that the uncertainty in the projections of ozone episode days stems mainly from the range of T_{max} projections in the CMIP5 ensemble. To test the robustness of our results, we repeat this analysis using the daily mean temperatures from CMIP5 instead of daily T_{max}. As shown in Figure S8, the changes in ozone episodes calculated in this way exhibit a similar spatial pattern as those calculated with T_{max} (Figure 3a), with an average of additional 1.9 d a^{-1} by the 2050s across the United States. The 90th and 10th percentile changes in ozone episodes as calculated using T_{max} from the 19 CMIP5 models are displayed in Figure S9.

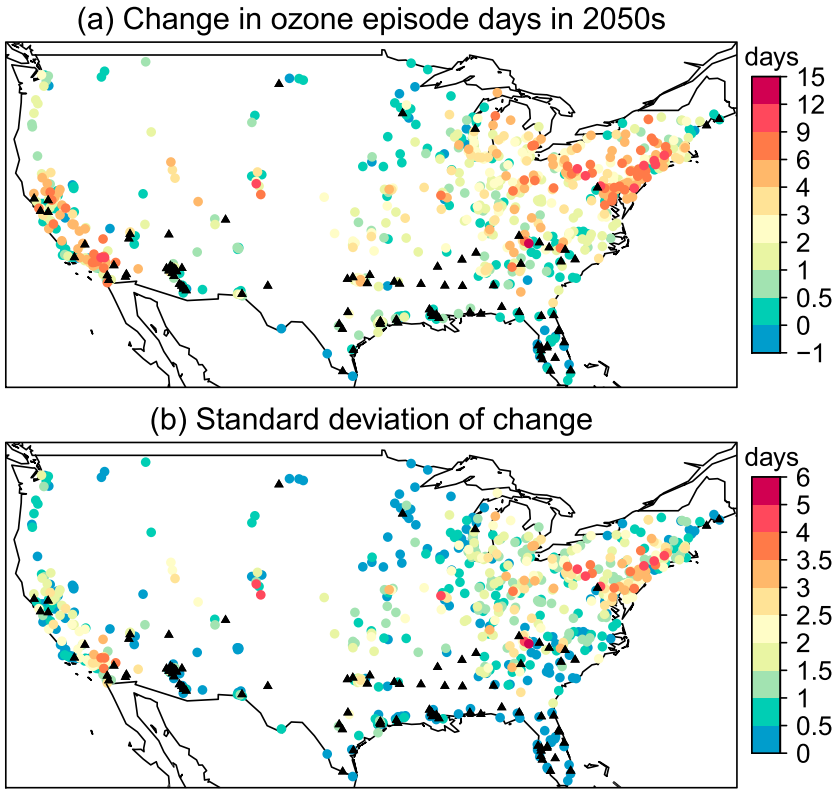

Figure 3. (a) Mean changes from 2000–2009 to 2050–2059 in ozone episode days due to climate change in the RCP4.5 scenario, as calculated using statistically downscaled projections of daily maximum temperatures from 19 CMIP5 models. (b) The standard deviation of the changes in ozone episode days across the 19 CMIP5 models at each site. The sites where the inclusion of T_{max} does not improve the EVT model for daily MDA8 ozone are denoted by black triangles.

6. Discussion and Conclusions

Using extreme value theory (EVT) and downscaled CMIP5 temperatures, we develop a hybrid-EVT model to examine the impact of 2000–2050 climate change on ozone episode days at 816 sites across the United States. We define an ozone episode day as those days when MDA8 ozone is greater than 75 ppbv and use daily T_{max} as the sole predictor. We first examine the stationarity of the ozone-temperature slopes using observed MDA8 ozone and daily T_{max} during the ozone season (May–September) from 2003 to 2012. At very high temperatures (above the 95th percentile), we find that 20% of U.S. sites exhibit a significant decrease in the ozone-temperature slope. Our study marks the first time such ozone suppression has been detected not just in California [*Steiner et al.*, 2010] but also in the Northeast, Southwest, and deep South.

Our hybrid-EVT model consists of two parts: (1) a point process model to simulate the ozone tails and (2) a logistic regression and a generalized Pareto distribution (GPD) model to capture the observed ozone suppression. Using this model, we find that observed and simulated ozone episode days closely correlate across the United States. Combining the model with future projections of statistically downscaled values for T_{max} from CMIP5 following the RCP4.5 scenario, we find that ozone episodes increase by 3–9 d a^{-1} in the Northeast, Midwest, and Southwest from 2000 to 2050 and by 0–2 days elsewhere. Our method assumes constant anthropogenic emissions at present-day levels, and the climate penalty we report considers only the influence of climate change on ozone episodes. Our results point to the need for ambitious emission controls to offset this penalty, especially in the Northeast and Southwest.

This study represents the first time that statistically downscaled meteorology from a large ensemble of climate models has been used to project future changes in ozone air quality. Using the median results of such an ensemble significantly decreases uncertainty in our projections. To our knowledge, this study is also the first to quantify the relationship of ozone and temperature in the United States using a hybrid-EVT model that takes into account ozone suppression at extremely high temperatures. Drawbacks of the model include its

assumption of constant anthropogenic emissions. The model also has difficulty predicting changes in ozone episodes in the deep South, where ozone and surface temperature exhibit relatively low correlation. Previous studies have shown that synoptic-scale phenomena such as the Bermuda High and the Great Plains low-level jet control MDA8 ozone variability in the South [e.g., *Shen et al*., 2015], but the influence of these phenomena on ozone episodes is unknown. Despite such limitations, the hybrid-EVT model promises to serve as a useful tool to rapidly assess the climate penalty on U.S. ozone air quality.

Acknowledgments

This work was supported by the NASA Air Quality Applied Sciences Team (NASA-MAP grant NNX13AO08G) and by the National Institute of Environmental Health Sciences (NIH grant R21ES022585). We thank the World Climate Research Programme's Working Group on Coupled Modelling, which oversees CMIP, and the modeling groups listed in Table S1. In partnership with the Global Organization for Earth System Science Portals, the DOE Program for Climate Model Diagnosis and Intercomparison provides coordinating support for CMIP and leads development of software infrastructure. We thank C.-Y. Cynthia Lin Lawell for her contributions.

References

Andrews, P. K., D. J. Chalmers, and M. Moremong (1992), Canopy-air temperature differences and soil water as predictors of water stress of apple trees grown in a humid, temperate climate, *J. Am. Soc. Hortic. Sci.*, *117*(3), 453–458.

Bloomer, B. J., J. W. Stehr, C. A. Piety, R. J. Salawitch, and R. R. Dickerson (2009), Observed relationships of ozone air pollution with temperature and emissions, *Geophys. Res. Lett.*, *36*, L09803, doi:10.1029/2009GL037308.

Camalier, L., W. Cox, and P. Dolwick (2007), The effects of meteorology on ozone in urban areas and their use in assessing ozone trends, *Atmos. Environ.*, *41*, 7127–7137, doi:10.1016/j.atmosenv.2007.04.061.

Chang, H. H., H. Hao, and S. E. Sarnat (2014), A statistical modeling framework for projecting future ambient ozone and its health impact due to climate change, *Atmos. Environ.*, *89*, 290–297.

Coles, S. G. (2001), *An Introduction to Statistical Modeling of Extreme Values*, Springer, New York.

Doherty, R. M., et al. (2013), Impacts of climate change on surface ozone and intercontinental ozone pollution: A multi-model study, *J. Geophys. Res. Atmos.*, *118*, 3744–3763, doi:10.1002/jgrd.50266.

Fiore, A. M., et al. (2009), Multimodel estimates of intercontinental source-receptor relationships for ozone pollution, *J. Geophys. Res.*, *114*, D04301, doi:10.1029/2008JD010816.

Gao, Y., J. S. Fu, J. B. Drake, J.-F. Lamarque, and T. Liu (2013), The impact of emission and climate change on ozone in the United States under representative concentration pathways (RCPs), *Atmos. Chem. Phys.*, *13*, 9607–9621, doi:10.5194/acp-13-9607-2013.

Gilleland, E., and R. W. Katz (2011), New software to analyze how extremes change over time, *Eos Trans. AGU*, *92*(2), 13–14, doi:10.1029/2011EO020001.

Guenther, A. B., P. R. Zimmerman, P. Harley, R. Monson, and R. Fall (1993), Isoprene and monoterpene emission rate variability: Model evaluations and sensitivity analyses, *J. Geophys. Res.*, *98*, 12,609–12,617, doi:10.1029/93JD00527.

Holloway, T., S. N. Spak, D. Barker, M. Bretl, C. Moberg, K. Hayhoe, J. Van Dorn, and D. Wuebbles (2008), Change in ozone air pollution over Chicago associated with global climate change, *J. Geophys. Res.*, *113*, D22306, doi:10.1029/2007JD009775.

Idso, S. B., R. J. Reginato, R. D. Jackson, and P. J. Pinter (1981), Foliage and air temperatures: Evidence for a dynamic "equivalence point", *Agric. Meteorol.*, *24*, 223–226.

Jacob, D. J., and D. A. Winner (2009), Effect of climate change on air quality, *Atmos. Environ.*, *43*, 51–63.

Kim, S.-W., A. Heckel, S. A. McKeen, G. J. Frost, E.-Y. Hsie, M. K. Trainer, A. Richter, J. P. Burrows, S. E. Peckham, and G. A. Grell (2006), Satellite-observed U.S. power plant NO_x emission reductions and their impact on air quality, *Geophys. Res. Lett.*, *33*, L22812, doi:10.1029/2006GL027749.

Lin, C.-Y. C., D. J. Jacob, and A. M. Fiore (2001), Trends in exceedances of the ozone air quality standard in the continental United States, 1980–1998, *Atmos. Environ.*, *35*, 3217–3228.

Maurer, E. P., and H. G. Hidalgo (2008), Utility of daily vs. monthly large-scale climate data: An intercomparison of two statistical downscaling methods, *Hydrol. Earth Syst. Sci.*, *12*, 551–563.

Meehl, G. A., and C. Tebaldi (2004), More intense, more frequent and longer lasting heat waves in the 21st century, *Science*, *305*, 994–997.

Mesinger, F., et al. (2006), North American regional reanalysis, *Bull. Am. Meteorol. Soc.*, *87*, 343–360.

Paternoster, R., R. Brame, P. Mazerolle, and A. Piquero (1998), Using the correct statistical test for the equality of regression coefficients, *Criminology*, *36*, 859.

Parrish, D. D., et al. (2014), Long-term changes in lower tropospheric baseline ozone concentrations: Comparing chemistry-climate models and observations at northern midlatitudes, *J. Geophys. Res. Atmos.*, *119*, 5719–5736, doi:10.1002/2013JD021435.

Porter, W. C., C. L. Heald, D. Cooley, and B. Russell (2015), Investigating the observed sensitivities of air-quality extremes to meteorological drivers via quantile regression, *Atmos. Chem. Phys.*, *15*, 10,349–10,366, doi:10.5194/acp-15-10349-2015.

Pfister, G. G., S. Walters, J.-F. Lamarque, J. Fast, M. C. Barth, J. Wong, J. Done, G. Holland, and C. L. Bruyère (2014), Projections of future summertime ozone over the U.S, *J. Geophys. Res. Atmos.*, *119*, 5559–5582, doi:10.1002/2013JD020932.

Rasulov, B., K. Hüve, I. Bichele, A. Laisk, and Ü. Niinemets (2010), Temperature response of isoprene emission in vivo reflects a combined effect of substrate limitations and isoprene synthase activity: A kinetic analysis, *Plant Physiol.*, *154*(3), 1558–1570.

Rieder, H. E., A. M. Fiore, L. M. Polvani, J. F. Lamarque, and Y. Fang (2013), Changes in the frequency and return level of high ozone pollution events over the eastern United States following emission controls, *Environ. Res. Lett.*, *8*(1), 014012, doi:10.1088/1748-9326/8/1/014012.

Rieder, H. E., A. M. Fiore, L. W. Horowitz, and V. Naik (2015), Projecting policy-relevant metrics for high summertime ozone pollution events over the eastern United States due to climate and emission changes during the 21st century, *J. Geophys. Res. Atmos.*, *120*, 784–800, doi:10.1002/2014JD022303.

Rasmussen, D. J., A. M. Fiore, V. Naik, L. W. Horowitz, S. J. McGinnis, and M. G. Schultz (2012), Surface ozone-temperature relationships in the eastern U.S.: A monthly climatology for evaluating chemistry-climate models, *Atmos. Environ.*, *47*, 142–153, doi:10.1016/j.atmosenv.2011.11.021.

Reclamation (2013), Downscaled CMIP3 and CMIP5 climate and hydrology projections: Release of downscaled CMIP5 climate projections, comparison with preceding information, and summary of user needs, prepared by the U.S. Department of the Interior, Bureau of Reclamation, Technical Services Center, Denver, Colorado, 47pp.

Sharkey, T. D., E. L. Singsaas, P. J. Vanderveer, and C. Geron (1996), Field measurements of isoprene emission from trees in response to temperature and light, *Tree Physiol.*, *16*(7), 649–654.

Shen, L., L. J. Mickley, and A. P. K. Tai (2015), Influence of synoptic patterns on surface ozone variability over the Eastern United States from 1980 to 2012, *Atmos. Chem. Phys.*, *15*, 10,925–10,938, doi:10.5194/acp-15-10925-2015.

Schlink, U., et al. (2003), A rigorous inter-comparison of ground-level ozone predictions, *Atmos. Environ.*, *37*(23), 3237–3253.

Steiner, A. L., A. J. Davis, S. Sillman, R. C. Owen, A. M. Michalak, and A. M. Fiore (2010), Observed suppression of ozone formation at extremely high temperatures due to chemical and biophysical feedbacks, *Proc. Natl. Acad. Sci. U.S.A.*, doi:10.1073/pnas.1008336107.

Sillman, S., and P. J. Samson (1995), Impact of temperature on oxidant photochemistry in urban, polluted rural, and remote environments, *J. Geophys. Res.*, *100*, 11,497–11,508, doi:10.1029/94JD02146.

Singsaas, E. L., and T. D. Sharkey (2000), The effects of high temperature on isoprene synthesis in oak leaves, *Plant, Cell Environ.*, *23*(7), 751–757.

Taylor, K. E., R. J. Stouffer, and G. A. Meehl (2012), An overview of CMIP5 and the experiment design, *Bull. Am. Meteorol. Soc.*, *90*, 485–498, doi:10.1175/BAMS-D-11-00094.1.

Wu, S., L. J. Mickley, E. M. Leibensperger, D. J. Jacob, D. Rind, and D. G. Streets (2008), Effects of 2000–2050 global change on ozone air quality in the United States, *J. Geophys. Res.*, *113*, D06302, doi:10.1029/2007JD008917.

Wu, J., Y. Zhou, Y. Gao, J. S. Fu, B. A. Johnson, C. Huang, Y.-M. Kim, and Y. Liu (2014), Estimation and uncertainty analysis of impacts of future heat waves on mortality in the eastern United States, *Environ. Health Perspect.*, *122*(1), 10.